Two-dimensional arrangements of magnetic nanoparticles

Abdelwahab Ghazali
Groupe de Physique des Solides, UMR 7588-CNRS, Universités Paris 6 & Paris 7, 75251 Paris 05, France

Jean-Claude Lévy
Laboratoire de Physique Théorique de la Matière Condensée, EA 2382, pôle MPQ, Université Paris 7, case 7020, 75251 Paris 05, France

(Received 17 December 2002; published 10 February 2003)

Arrangements of magnetic nanoparticles in a plane interacting through hard core repulsion and magnetic dipole-dipole interaction are deduced from Monte Carlo relaxations. At low density, magnetic particles are arranged in sinuous lines and rings, while at higher densities lines of magnetic moments aggregate in spirals and vortices. An in-plane magnetic field tends to make lines parallel to the field and to break rings, while a perpendicular-to-the-plane field tends to arrange the particles in a glassy state.

DOI: 10.1103/PhysRevB.67.064409 PACS number(s): 75.75.+a, 75.25.+z, 75.80.+q

Recently the interest in magnetic nanoparticles for applications has been increasing considerably with the celebrated cases of ferrofluids[1] and magnetic recording.[2] Numerous physical and chemical techniques are presently available to prepare nanoparticles with rather well selected sizes.[3] The abundance and diversity of fabrication provides further comparative studies.

The observed arrangements of these particles in many experiments exhibit peculiar organizations in space, such as chains,[4] branched chains,[5] or even separate particles,[6] depending on the intensity and orientation of the applied magnetic field. So the existence of these structures deserves to be understood. From the theoretical point of view, the basic interactions between magnetic grains are quite simple: repulsive hard core interactions which prevent the particle condensation, and magnetic anisotropic dipole-dipole interactions which lead to these structures. The competition between the contact interactions and long range dipolar interactions has attracted many interesting works with extensive numerical studies.[7] Lines and rings were obtained in these approaches. Another interest in these structures comes from the curious interplay between the geometric and magnetic structures they offer. This remark leads us to note the similarity between magnetic nanoparticle systems and the spin lattice systems.[8]

Here we focus our interest on two-dimensional samples confined in a given area. This can easily be realized experimentally by different means such as surface confinement, surface deposition, or implantation in a quasi-two-dimensional medium.[9] Dipole-dipole interactions are known to lead to very complex magnetic structures in finite 3D samples.[10] For these samples, intricate fractal-like magnetic domain structures have been observed,[10] and theoretical approaches have been proposed.[11]

It is known experimentally that magnetic particles exhibit a slow relaxation and the equilibrium is not usually reached, so spin-glass configurations have been observed[12] with aging properties.[13] The particle energy in our Monte Carlo (MC) simulations reveals the effective state of bonding and also the elastic and dynamic properties of magnetic particle systems in a simple and transparent way. This is not easily deduced from experiments.

The particles are specified by their center position and their magnetization. The particle-particle interaction has two components: (i) the repulsive interaction: $H=\Sigma_{ij}V_{ij}$, where

$$V_{ij}=A\left[\frac{\|\vec{r_j}-\vec{r_i}\|}{\sigma}\right]^{-n} \quad \text{for} \quad \|\vec{r_j}-\vec{r_i}\|=r_{ji}<\sigma,$$

and

$$V_{ij}=0 \quad \text{for} \quad r_{ji}>\sigma. \tag{1}$$

We have taken for V_{ij} a power law with the exponent $n=8$; A is the repulsive intensity within an excluded sphere of grain diameter σ; and (ii) the dipole-dipole interaction:

$$H_{dip}=D\sum_{ij}\left(\frac{\vec{M}_i\cdot\vec{M}_j}{r_{ij}^3}-3\frac{(\vec{M}_i\cdot\vec{r}_{ij})(\vec{M}_j\cdot\vec{r}_{ij})}{r_{ij}^5}\right). \tag{2}$$

Here D is the dipolar coupling constant, and hereafter the dipolar energy D/σ^3 is taken as the energy unit. Under an applied magnetic field $\vec{H}$, the Zeeman interaction reads

$$H_{Ze}=-\sum_i \vec{H}\cdot\vec{M}_i. \tag{3}$$

Our MC process starts from random positions of particles within a disk of diameter 70σ. The particles hold randomly oriented magnetic moments on the unit radius sphere. Then the following configurations are obtained from random spatial excursions within a disk of diameter $\alpha\sigma$ with $\alpha\ll 1$, and random reorientations of the magnetization moments on the unit sphere. They are relaxed according to the MC process at the temperature $k_BT=0.1$ expressed in the dipolar energy unit. The moderate temperature we choose allows spin variations and displacements small enough to maintain short

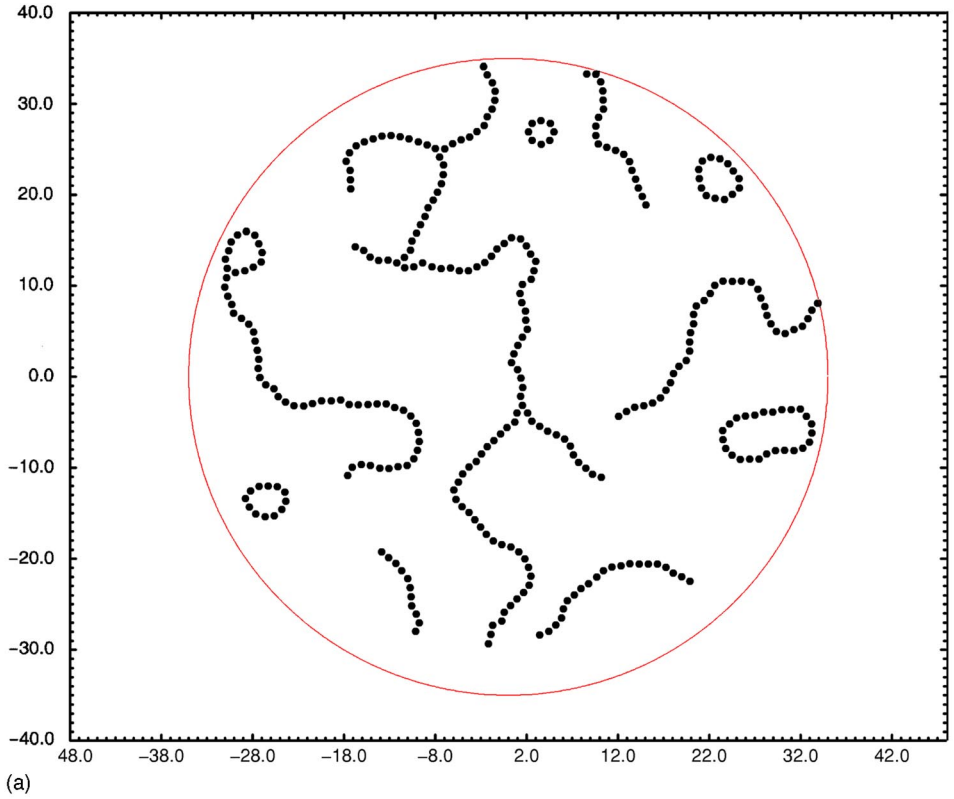

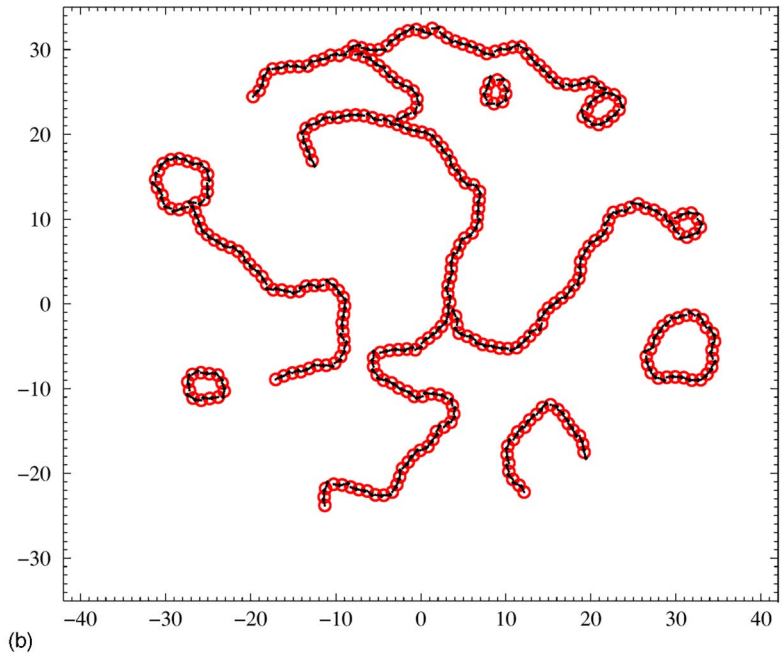

FIG. 1. Snapshots of 331 particles confined within a disk of diameter 70σ: (a) after 3×10^6 MC steps, and (b) after 6×10^6 MC steps with the magnetic moments, shown by arrows.

range magnetic interactions but large enough to ensure relaxation. The confinement is a mere rejection of MC displacements out of the disk.

During the MC relaxation, the energy is soon stabilized, but the configuration evolves slowly. This relaxation slowing down is due to the weakness of long range dipolar interactions, especially at low particle densities. Various configurations are shown in the following. They are taken at different stages of relaxation in order to visualize the basic trends of the space and spin evolutions.

The low density sample with 331 particles of diameter σ is confined within a disk of diameter 70σ. Figures 1(a) and 1(b) show configuration snapshots taken, respectively, after 3×10^6 and 6×10^6 MC steps, with the magnetic configuration corresponding to Fig. 1(b). Figure 1(a) presents five rings, one linked with a chain, and six chains, while Fig. 1(b)

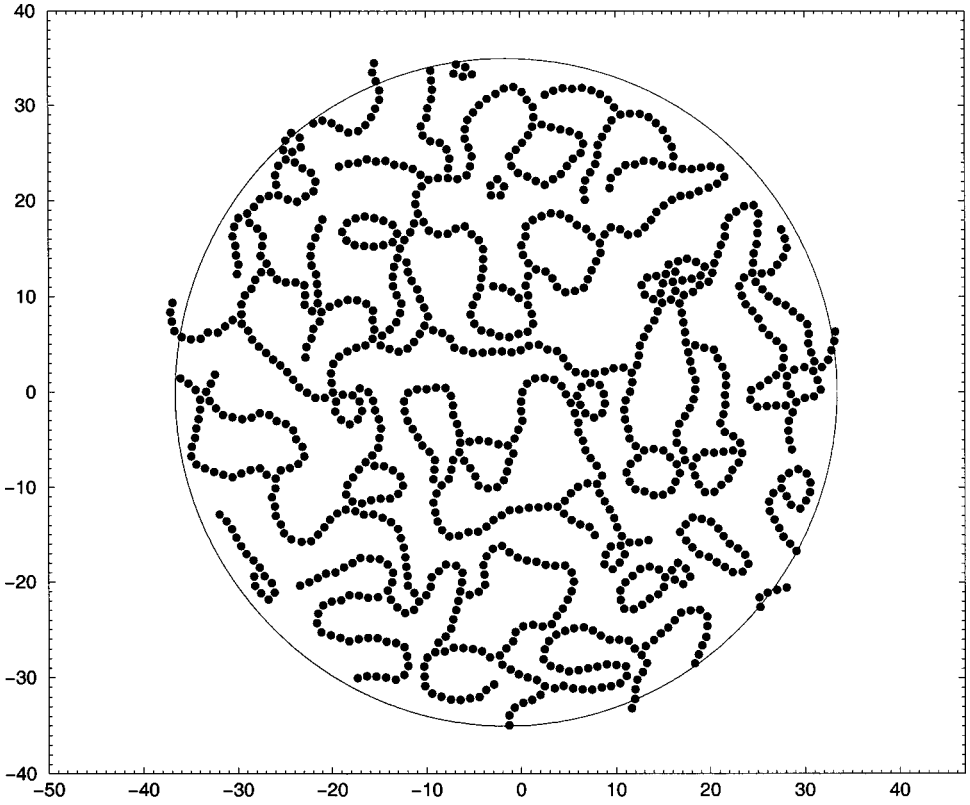

FIG. 2. A snapshot of 1031 particles after 2×10^5 MC steps.

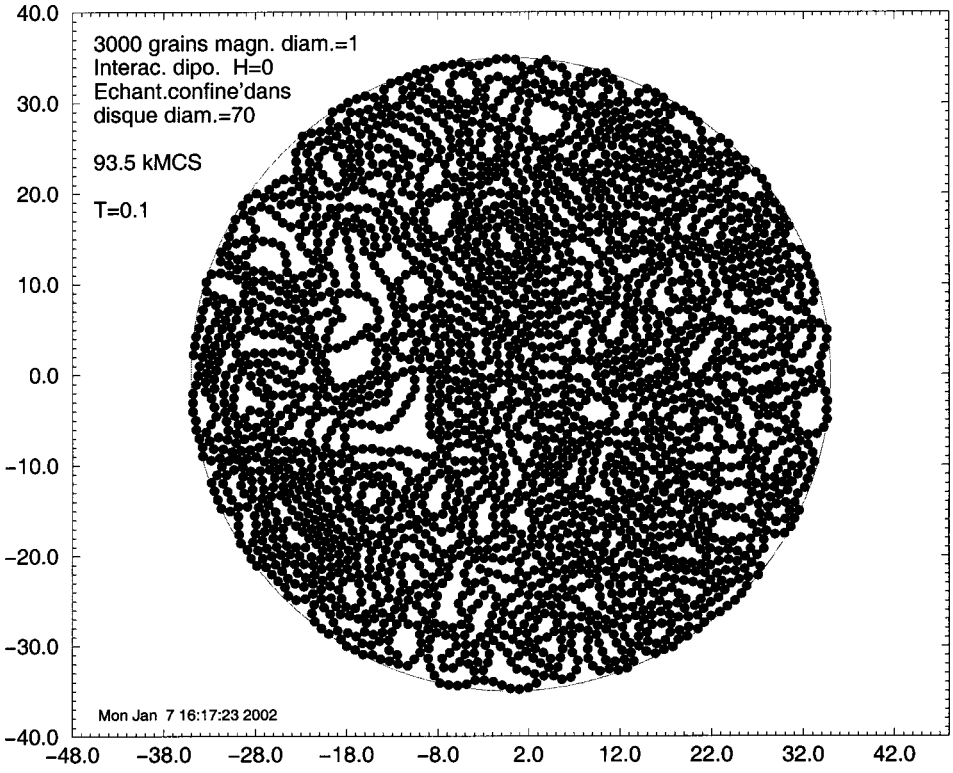

FIG. 3. A snapshot of 3000 particles after 9.35×10^4 MC steps.

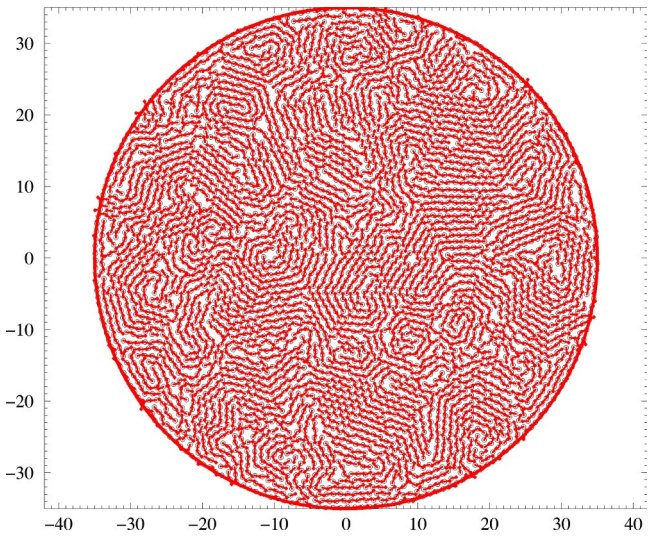

FIG. 4. A snapshot of 4000 particles after 7×10^4 MC steps with the magnetic moments shown by arrows. Note that the magnetic vortices are centered on voids.

presents three independent rings, two rings linked with a chain and three chains. The dipole-dipole coupling favors straight lines which can be curved due to temperature. The energy loss due to the curvature of rings is balanced by the energy gain due to the closure of ending connections. The magnetic structure shown in Fig. 1(b) confirms this. Dipoles are always aligned along the chain. The energy per site is close to $\zeta(3)=1.2$ units, where $\zeta(s)$ is the Riemann zeta function. It corresponds to a connectivity of just two nearest neighbors.

The second sample is more dense, it contains 1031 particles with the coverage of about 20%. This sample is relaxed after 2×10^5 MC steps. It contains three separate rings, six separate chains, and 23 rings linked with a chain, as shown in Fig. 2. The energy per site is close to 1.3 units, which corresponds to a connectivity two, as before. The new feature is the abundance of rings linked with chains and more generally the appearance of the branching phenomenon which increases the binding energy of the branching site by about 0.3 units.

The third sample contains 3000 particles within the disk. The coverage is about 60%. After MC steps, the sample is rather relaxed, even if the density is not homogeneous, as seen in Fig. 3. The energy per site is still close to 1.4 units, which corresponds to a connectivity of 2, exactly as for lower densities. The structure is made of almost parallel laces which weakly interact together. This weak effective interaction explains the lack of density homogenization. The magnetic structure of the sample displays magnetic vortices, the centers of which are vacancies shown in Fig. 3. These are the singular points of the magnetization distribution.

These features are expected to lead to a very specific elastic behavior and to peculiar dynamic properties connected with the weakness of the bulk modulus and shear deformation for confined or unconfined samples. Chain and ring vibrations as well as vortex deformations require a weak excitation energy and thus occur at low frequencies, leading to a viscous-type behavior.

The fourth sample contains 4000 particles within a disk of the same diameter 70σ. It is thus close to the complete coverage; see the snapshot in Fig. 4 after 7×10^4 MC steps. This sample is clearly polycrystalline, and contains numerous

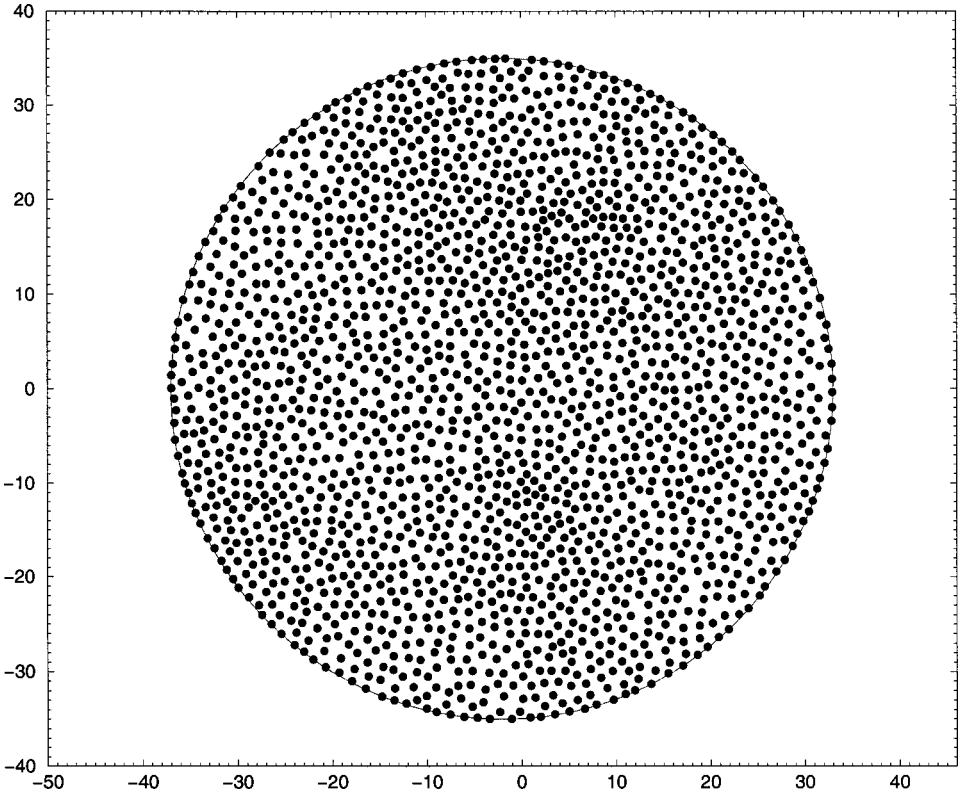

FIG. 5. A snapshot of 2000 particles with an out-of-plane field after 6×10^4 MC steps.

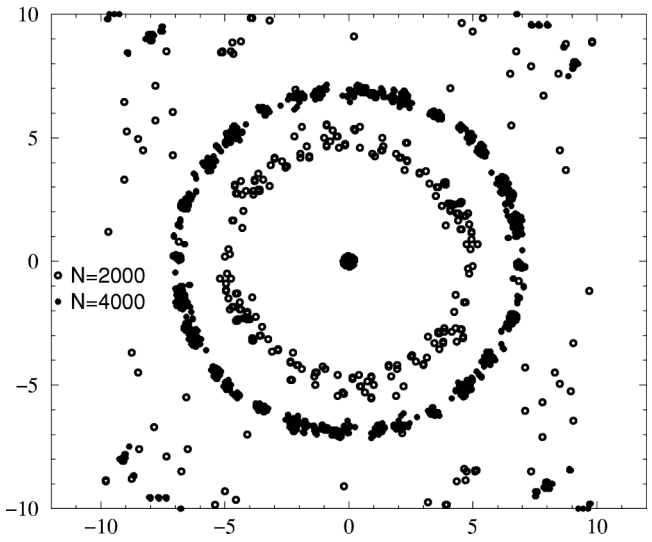

FIG. 6. Fourier transforms of 2000 and 4000 particles with a saturating out-of-plane field after 6×10^4 MC steps. Notice the thick rings.

point defects and grain boundaries. As before, the magnetic structure shown in Fig. 4 indicates that numerous magnetic vortices are present and centered at lattice vacancies. The energy per site is still close to 1.5 units, not far from a connectivity of 2, as before in spite of the compact crystalline structure. As in the case of medium densities, the magnetic vortices associated with lattice defects are stable.

For comparison, the dipole-dipole energy per site in a triangular lattice with a lattice parameter of 1 and a ferromagnetic arrangement parallel to one triangle side is -2.63 for a 200×200 sample.[8] The site energy for the various samples lies between this value and $\zeta(3)=1.2$. This proves that the equilibrium is not yet reached but the energy evolution is rather slow.

An in-plane magnetic field applied to a stable structure with lines and rings tends to make lines parallel to the magnetic field and to break the rings. Such structural changes are expected to depend on the density, magnetic field intensity, and temperature. This was studied by many authors in two and three dimensions, experimentally and numerically.[14] Because of the slow relaxation process, this transition also depends on the starting configuration, as shown both experimentally and numerically. With a random initial configuration, nanoparticles are easily aligned along the magnetic field, and straight chains grow. With an initial zero-field relaxed structure, rings exist at the very beginning and are lately broken when a strong enough field is applied after a long enough time. In both cases the elastic and dynamic properties are locally anisotropic.

A magnetic field normal to the plane has quite a different effect: separate nanoparticles align their magnetization parallel to this field in the same direction. Thus the dipole-dipole interaction between particles is repulsive. For a large enough field there are no more lines or rings whatever the initial configuration. In Fig. 5 the configuration of a sample of 2000 particles submitted to an external normal field of magnitude $H_z=7$ is shown after 6×10^4 MC steps. No perfect crystalline configuration is obtained. A similar configuration occurs for sets of magnetic or electric dipoles perpendicular to the surface plane[6,15]

It is interesting to note that the repulsive site dipolar interactionenergy in a triangular lattice is $+5.363$, and the site dipolar energy in a simple square lattice with the same density is $+5.452$. The smallness of the difference between these two results comes from the balance between fewer neighbors but closer ones for a square lattice, and more neighbors but further ones for a triangular lattice. It makes possible distortions such as those observed in Fig. 5 and also in experiments.[6,15] This amorphous arrangement with many local configurations is well illustrated by the diffraction patterns of MC configurations reported in Fig. 6, where thick rings appear even at a high particle density. Another consequence is the transition from a triangular array of nanoparticles to a square arrangement.[16] Many local rearrangements occur in this noncrystalline structure.

[1] R.W. Chantrell, A. Bradbury, J. Popplewell, and S.W. Charles, J. Phys. A **13**, L119 (1980); R. E. Rosensweig, *Ferrohydrodynamics* (Dover, New York, 1997).
[2] D. Kechrakos and K.N. Trohidou, Phys. Rev. B **62**, 3941 (2000).
[3] C. Petit, A. Taleb, and M.P. Pileni, J. Mater. Sci. **103**, 1805 (1999); Ph. Toneguzzo *et al.*, J. Mater. Sci. **35**, 3767 (2000).
[4] C.-Y. Hong, I.J. Jang, H.E. Horng, C.J. Hsu, Y.D. Yao, and H.C. Yang, J. Appl. Phys. **81**, 4275 (1997); W. Wen, F. Kun, K.F. Pal, D.W. Zheng, and K.N. Tu, Phys. Rev. E **59**, R4758 (1999).
[5] L. Zhang and A. Manthiram, Appl. Phys. Lett. **70**, 2469 (1997).
[6] V. Petukhov, V. Zhikharev, M. Ibragimova, E. Zheglov, V. Bazarov and I. Khaibullin, Solid State Commun. **97**, 361 (1996).
[7] J.J. Weis and D. Levesque, Phys. Rev. Lett. **71**, 2729 (1993); Y. Ishii, J. Phys. Soc. Jpn. **67**, 3050 (1997).
[8] E.Y. Vedmedenko, A. Ghazali, and J.-C.S. Lévy, Phys. Rev. B **59**, 3329 (1999).
[9] M. Golosovsky, Y. Saado, and D. Davidov, Appl. Phys. Lett. **75**, 4168 (1999).
[10] C. Guillaud and R. Vautier, in *Colloque National de Magnétisme* (C.N.R.S., Paris, 1958), p. 24.
[11] I. Privorotskii, *Thermodynamic Theory of Domain Structures* (Wiley, New York, 1976).
[12] L. Del Bianco, A. Hernando, E. Bonetti, and E. Navarro, Phys. Rev. B **56**, 8894 (1997).
[13] H. Mamiya, I. Nakatani, and T. Furubayashi, Phys. Rev. Lett. **82**, 4332 (1999).
[14] F. Kun, W. Wen, K.F. Pal, and K.N. Tu, Phys. Rev. E **64**, 061503 (2001).
[15] M. Saint-Jean, C. Even, and C. Guthmann, Europhys. Lett. **55**, 45 (2001).
[16] B. Abou, J.-E. Weisfred, and S. Roux, J. Fluid Mech. **416**, 217 (2000).